Additional file 1

Sample collection and plasma processing

For plasma separation, 2–10 mL of peripheral blood was collected into Cell-Free DNA Storage Tubes (CWBIO, Jiangsu, China) or EDTA anticoagulant tubes (Hebei Kangweishi Medical Technology, Hebei, China). For gDNA extraction without plasma separation, 1–5 mL peripheral blood was collected in EDTA anticoagulant tubes. Plasma was separated within the manufacturer-recommended stability window by centrifugation at 1,600g for 10 min at 4 °C, followed by a second centrifugation at 16,000g for 10 min at 4 °C to remove residual cellular debris. Plasma was aliquoted into 2-mL cryovials and stored at −80 °C until cfDNA extraction.

cfDNA and gDNA extraction

cfDNA was extracted from plasma using the Apostle MiniMax™ High Efficiency cfDNA Extraction Kit (Apostle Inc., San Jose, CA) and eluted in 30 µL. cfDNA concentration was quantified using the Qubit™ 1X dsDNA HS Assay Kit (Thermo Fisher Scientific, Wilmington). gDNA was extracted from buffy coat or peripheral blood using the Lab-Aid 824 automated nucleic acid extraction system and matched extraction reagents (Zeesan Biotech, Xiamen, China). Where indicated, gDNA was fragmented to approximately 160 bp by sonication using a Covaris M220 ultrasonicator (Covaris, Inc., MA).

MMCA assay for SNP genotyping

To genotype the 96-SNP panel, its two functional subsets (48 *HBB*-flanking SNPs and 48 genome-wide SNPs) were each divided into four reactions, resulting in a total of eight MMCA reactions. Each reaction was performed in 25-µL reactions containing 1× PCR master buffer, 7.0 mM $MgCl_2$, 0.4 mM dNTP mixture, 2.0 U *Taq* HS DNA polymerase (Accurate Biology, Hunan, China), 0.25 U uracil-N-glycosylase (Thermo Fisher Scientific), 2–6 µM Tag primer, 0.016–0.15 µM tailed primers, 0.32–1.6 µM fluorescent probes and 5 µL of human gDNA (approximately 1 ng/µL) or water control.

PCR amplification and melting curve analysis were performed on a SLAN-96S real-time PCR instrument (Hongshi Medical Technology, Shanghai, China). The thermal profile was 50 °C for 2 min and 95 °C for 5 min, followed by 6 cycles of 95 °C for 15 s, 53 °C for 15 s and 76 °C for 20 s; 55 cycles of 95 °C for 15 s, 58 °C for 15 s and 76 °C for 20 s; and melting analysis after 95 °C for 1 min and 37 °C for 3 min, with temperature increasing from 40 °C to 85 °C at 0.04 °C per step. Fluorescence from five detection channels (FAM at 510 nm, HEX at 565 nm, ROX at 620 nm, Cy5 at 665 nm, Quasar 705 at 705 nm) was recorded during annealing in the second amplification stage and throughout melting analysis. SNP genotypes were assigned from allele-specific melting peak patterns.

Drop-Phase assay for experimental haplotype phasing

The Drop-Phase assay was used to experimentally determine linkage between SNP alleles and *HBB* mutation-site alleles. Reactions were performed in 30 µL containing 1× supermix (TargetingOne, Beijing, China), 800 nM primers, 250 nM probes and 1 µL of human gDNA (approximately 10 ng/µL). PCR was performed on an A300 Fast Thermal Cycler (Longgene, Hangzhou, China) as follows: 95 °C for 10 min; 40 cycles of 94 °C for 30 s and 54 °C for 1 min; and 12 °C for 5 min. Droplet generation and fluorescence detection were performed using the TargetingOne Droplet Digital PCR System. SNP alleles were assigned to mutant- or wild-type–associated *HBB* haplotypes according to the enrichment of double-positive droplets containing both SNP and *HBB* mutation-site allele signals above the expected background of random co-partitioning.[1]

Multiplex preamplification of cfDNA

A multiplex preamplification assay was performed to enrich all SNP loci and *HBB* mutation sites before allele quantification. Each 50-µL reaction contained 1× PCR master buffer, 5.0 mM $MgCl_2$, 0.3 mM dNTP mixture, 4.0 U *Taq* HS DNA polymerase, 40 nM primers and 25 µL cfDNA template. Thermal cycling was performed as follows: 95 °C for 5 min; 10 cycles of 95 °C for 20 s, 58 °C for 2 min and 72 °C for 2 min; and final extension at 72 °C for 2 min.

Allele quantification by dPCR

Allele quantification assays were performed in 30-µL reactions containing 1× supermix, 800 nM primers, 250 nM probes and 1 µL preamplified cfDNA product. PCR was performed on an A300 Fast Thermal Cycler as follows: 95 °C for 10 min; 40 cycles of 94 °C for 30 s and 58 °C for 1 min; and 12 °C for 5 min. Droplet generation and detection were performed on the TargetingOne Droplet Digital PCR System. Absolute copy numbers were calculated for each allele. For all SNP and mutation allele quantification assays, the limit of blank (LOB) was determined using preamplified products generated from 5 ng sheared gDNA per reaction, using 20 replicate blank measurements per assay. The LOB was calculated as the one-sided 95% upper limit of the blank distribution, LOB = mean + 1.645 × SD, where mean and SD denote the mean and the standard deviation of the blank measurements; the LOB therefore represents the highest signal expected from a blank sample with 95% probability. It is a prediction limit for an individual blank measurement and should not be confused with a confidence interval for the mean blank signal.

Linkage decay analysis
Eight SNPs (rs7484061, rs6421049, rs2187610, rs6578588, rs4910543, rs10128556, rs7480197, rs74049345) were paired with the reference SNP rs7938317 to generate eight Drop-Phase assays spanning genomic distances of 5,928, 11,814 bp, 23,191, 30,036, 36,612, 41,468, 46,119, 50,580 bp, respectively. Each Drop-Phase assay was performed in triplicate using gDNA, and the linkage percentage was calculated from the proportion of linked molecules. The LOB was determined using a Drop-Phase assay pairing *RPP30* with rs7938317, which are located on different chromosomes, with gDNA tested in 20 replicates, using the same one-sided 95% definition as the allele quantification assays described above (LOB = mean + 1.645 × SD).

FF estimation
FF was estimated using FF-iSNPs allele-resolved dPCR copy numbers across "n" loci [Equation (1)]. Measurement error was assessed as the standard deviation (σ) of repeated estimates and compared with the Poisson noise expected from the DNA input used in the preamplification reaction [Equation (2)].[2]

$$Fetal\ fraction\ (FF) = \frac{1}{n} \times \sum_{i=1}^{n} \frac{2 \times C_{paternal\ specific\ allele}}{C_{paternal\ specific\ allele} + C_{maternal\ specific\ allele}} \quad \text{Equation (1)}$$

where C indicates the copy number reported by dPCR.

$$\sigma_{FF-Poisson} = \sqrt{\left(\frac{2 * Fetal\ fraction}{input\ DNA\ in\ preamp}\right)} \quad \text{Equation (2)}$$

Paternal mutation inference
Paternal inheritance was determined by direct mutation detection when parental mutations differed, or by Pat-iSNP linkage when they were identical. A Z-score was calculated from allele counts and the variance derived from the LOB [Equation (3)].[3] A Z-score ≥ 3 indicated inheritance of the paternal-specific allele, whereas a Z-score ≤ 0 indicated non-inheritance. Intermediate values (0 < Z < 3) satisfied neither rule and were classified as inconclusive.

$$Z = [C_{paternal\ specific\ allele} / (C_{paternal\ specific\ allele} + C_{shared\ allele\ of\ parents}) - LOB] / \sigma \quad \text{Equation (3)}$$

where C denotes the detected copy number, LOB denotes the limit of blank, and σ denotes the standard deviation of the blank measurements used to derive the LOB.

Maternal mutation inference
For maternal mutation inference, we applied a quantitative framework based on the binomial LLR integrated with the SPRT. This strategy was applied to Mat-iSNPs and the maternal mutation site itself. All allele counts ($C_{M,i}$ and $C_{W,i}$, representing the detected copy number of mutant-linked and wild-type–linked alleles, respectively) were converted to numbers of independent original molecules before being used in Equation (4), as follows. Preamplified copies are not independent original molecules, so the raw dPCR counts cannot be used directly: inserting them would overstate the amount of independent information available and inflate the LLR. N, the number of independent original molecules available for inference at a locus, was therefore estimated from the cfDNA input. The cfDNA concentration measured by Qubit fluorometry gave the mass of cfDNA added to the preamplification reaction, which was converted to haploid genome equivalents using 3.3 pg per haploid genome. At each locus, the detected counts were then rescaled so that the summed mutant-linked and wild-type–linked counts equal N. This rescaling preserves the mutant-to-wild-type allelic ratio measured by dPCR while setting N to the number of independent molecules actually sampled. N enters Equation (4) through the counts: because each single-locus term is proportional to the counts, the cumulative LLR scales approximately linearly with N, and N therefore determines how rapidly λ separates the two hypotheses and reaches the ±4.595 decision boundaries. Locus-specific amplification efficiency was not corrected individually, because both alleles at a locus are co-amplified in the same reaction and the LLR depends on their ratio; rescaling therefore leaves the allelic ratio unchanged while determining N.

For each informative locus i, the expected proportion of the mutant-linked allele (M) in maternal plasma was defined under two competing hypotheses. Null hypothesis (H_0): The fetus did not inherit the maternal mutant haplotype. Alternative hypothesis (H_1): The fetus inherited the maternal mutant haplotype.

Based on whether the inherited paternal allele is identical to the maternal mutant allele or to the maternal wild-type allele, two scenarios were considered. If the inherited paternal allele matches the maternal mutant allele, then $p_0 = 0.5$ and $p_1 = 0.5 + FF/2$. Conversely, if the inherited paternal allele matches the maternal wild-type allele, then $p_0 = 0.5 - FF/2$ and $p_1 = 0.5$.
The cumulative LLR (λ) across m informative loci was calculated as:

$$\lambda = \sum_{i=1}^{m} [C_{M,i} * \ln\left(\frac{p_{1,i}}{p_{0,i}}\right) + C_{W,i} * \ln\left(\frac{1-p_{1,i}}{1-p_{0,i}}\right)] \quad \text{Equation (4)}$$

Wald's SPRT framework was applied with predefined type I (α) and type II (β) error rates of 0.01, yielding decision boundaries of $\pm\ln(99) \approx \pm 4.595$; $\lambda \geq 4.595$: classified as maternal mutant haplotype inherited; $\lambda \leq -4.595$: classified as maternal wild-type haplotype inherited; $-4.595 < \lambda < 4.595$: classified as inconclusive, prompting either additional informative loci or a repeated blood draw.

Paternal mutation inference in the absence of informative Pat-iLoci

When both parents carried the same pathogenic variant and no Pat-iLocus was available, paternal transmission could not be resolved by direct detection of a paternal-specific allele or by Pat-iSNP linkage analysis. Inference was then made from the dosage of the shared mutation in maternal plasma. This test uses the same binomial LLR–SPRT framework described above for the maternal mutation site, with the roles of the two parents exchanged.

Maternal inheritance was resolved first, from the Mat-iSNPs and the maternal mutation site, using Equation (4) with the scenario-specific values of p_0 and p_1 given above. Once the maternally transmitted allele was known, it played the part that the paternally transmitted allele plays in maternal inference: it fixed which pair of expected mutant-allele proportions was to be contrasted. Two hypotheses were then compared at the mutation site. Under the null hypothesis (H_0) the fetus did not inherit the paternal mutant allele; under the alternative hypothesis (H_1) it did. The expected proportion of the mutant allele (p) in maternal plasma was:

If the maternal mutation was inherited, then $p_0 = 0.5$ and $p_1 = 0.5 + FF/2$. Conversely, if the maternal mutation was not inherited, then $p_0 = 0.5 - FF/2$ and $p_1 = 0.5$.

The four expected proportions are therefore the same as those used for the maternal mutation site, with the parental roles exchanged: 0.5 − FF/2 corresponds to a fetus carrying no copy of the shared mutation (N/N), 0.5 to a heterozygous fetus (M/N), and 0.5 + FF/2 to a fetus homozygous for the shared mutation (M/M).

Substituting these values into Equation (4) with a single informative locus (m = 1) gives the log-likelihood ratio

$$\lambda = [C_M * \ln\left(\frac{p_1}{p_0}\right) + C_W * \ln\left(\frac{1-p_1}{1-p_0}\right)] \qquad \text{Equation (5)}$$

which was interpreted with the same SPRT boundaries as the maternal inference (type I and type II error rates of 0.01): $\lambda \geq 4.595$ indicated inheritance of the paternal mutation, $\lambda \leq -4.595$ indicated non-inheritance, and $-4.595 < \lambda < 4.595$ was classified as inconclusive, prompting a repeated blood draw.

Turnaround-time and cost analysis

Turnaround time was calculated from extracted parental gDNA and maternal plasma cfDNA to final genotype interpretation and included MMCA genotyping, Drop-Phase phasing, multiplex preamplification, dPCR allele quantification and data analysis. Cost estimates included assay reagents and consumables for parental genotyping, phasing and cfDNA analysis, but excluded labour, equipment depreciation and general laboratory overheads unless otherwise stated.

Cumulative recombination probability calculation

Cumulative recombination probability was estimated by summing the recombination probabilities across all adjacent informative SNP pairs in a given set of loci. For each SNP pair, the recombination probability was derived from the genetic distance (cM), which was calculated as the physical distance (Mb) multiplied by the recombination rate (cM/Mb) of the corresponding genomic interval. Recombination rates for each interval were obtained from the deCODE recombination map. The cumulative probability across all interrogated loci was then used as an indicator of the overall recombination risk. This cumulative estimate follows the same genetic-distance-based principle used in the HMM transition probability of Chen et al.,[4] but was applied here as an independent risk metric rather than as part of a hidden Markov model. In this study, a cumulative recombination probability exceeding 0.01 was considered high and prompted caution in interpretation.

Validation of linkage inference

To validate linkage accuracy, we analyzed a β-thalassemia high-risk pedigree for which parental and offspring gDNA were available. The mother carried the *HBB*:c.126_129delCTTT heterozygous mutation and the father carried the *HBB*:c.216_217insA heterozygous mutation. A duplex Drop-Phase assay combining *HBB*:c.216_217insA with four SNP loci reconstructed the paternal mutant-linked haplotype. The inferred offspring SNP genotypes were fully concordant with MMCA genotyping results (Figure S10 and Table S1), confirming the accuracy of Drop-Phase–based linkage inference.

Representative family analysis

A representative family (Sample-59) was selected to illustrate the complete analytical workflow. Both parents carried the *HBB*:c.126_129delCTTT mutation, representing the most challenging inference scenario in which parental origin cannot be resolved by direct mutation detection alone. MMCA-based SNP genotyping identified 16 Pat-iLoci, 6 Mat-iLoci and 7 FF-iSNPs. One Pat-iSNP (rs10768682) and three Mat-iSNPs (rs34220818, rs7484061 and rs10837631) were selected for linkage analysis and haplotype reconstruction (Figure S19A, B). dPCR-based quantification of maternal plasma cfDNA yielded an FF of 6.33% (Figure S18A–C). For paternal inference, the paternal-specific allele fraction was 0.16%, and Z-score analysis indicated non-inheritance of the paternal wild-type–linked allele ($Z = -1.18$), supporting inheritance of the paternal mutant-linked haplotype (Figure S19C, D). For maternal inference, SPRT analysis of the three Mat-iSNPs yielded λ values of 21.02, 12.27 and 13.68, whereas the

HBB:c.126_129delCTTT mutation site yielded a λ value of 16.12 (Figure S18D). The cumulative λ value of 63.09 provided strong statistical evidence for inheritance of the maternal mutant-linked haplotype (Figure S18 and Figure S19).

Reference

1. Regan JF, Kamitaki N, Legler T, Cooper S, Klitgord N, Karlin-Neumann G, et al. A rapid molecular approach for chromosomal phasing. PLoS One. 2015;10(3):e0118270.
2. Camunas-Soler J, Lee H, Hudgins L, Hintz SR, Blumenfeld YJ, El-Sayed YY, et al. Noninvasive Prenatal Diagnosis of Single-Gene Disorders by Use of Droplet Digital PCR. Clinical Chemistry. 2018;64(2):336–45.
3. Zhang JL, Li JL, Saucier JB, Feng YM, Jiang YJ, Sinson J, et al. Non-invasive prenatal sequencing for multiple Mendelian monogenic disorders using circulating cell-free fetal DNA. Nat Med. 2019;25(3):439–+.
4. Chen C, Li R, Sun J, Zhu Y, Jiang L, Li J, et al. Noninvasive prenatal testing of α-thalassemia and β-thalassemia through population-based parental haplotyping. Genome Med. 2021;13(1):18.

Supplementary Figures

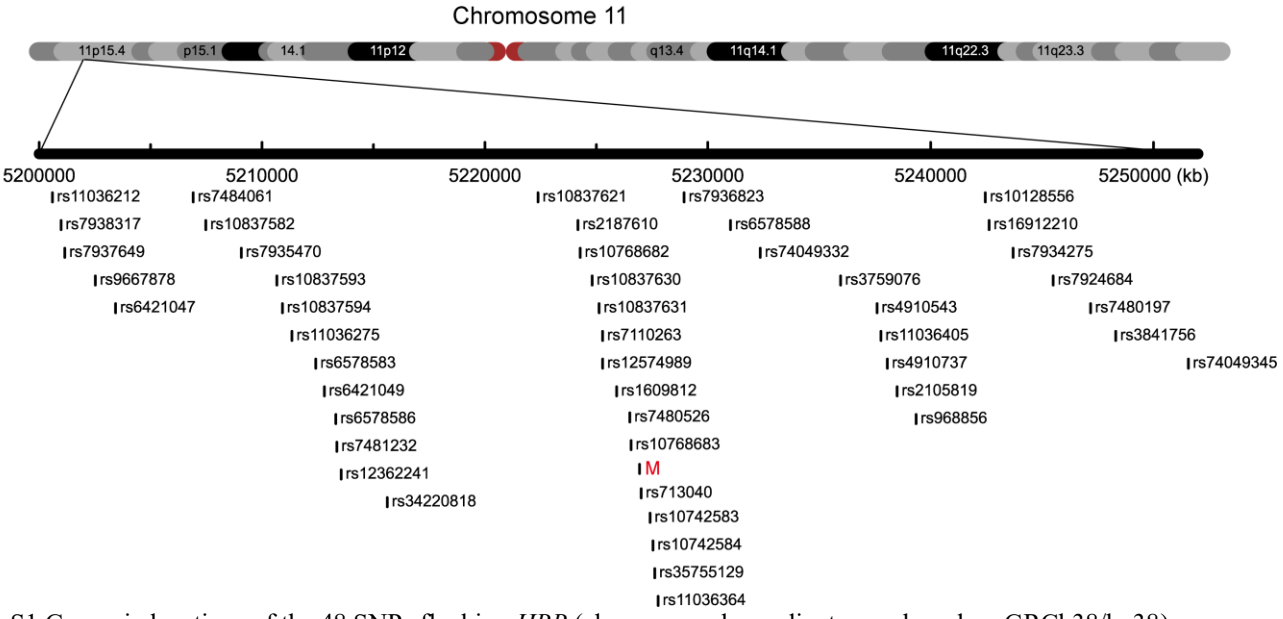


Figure S1 Genomic locations of the 48 SNPs flanking *HBB* (chromosomal coordinates are based on GRCh38/hg38).

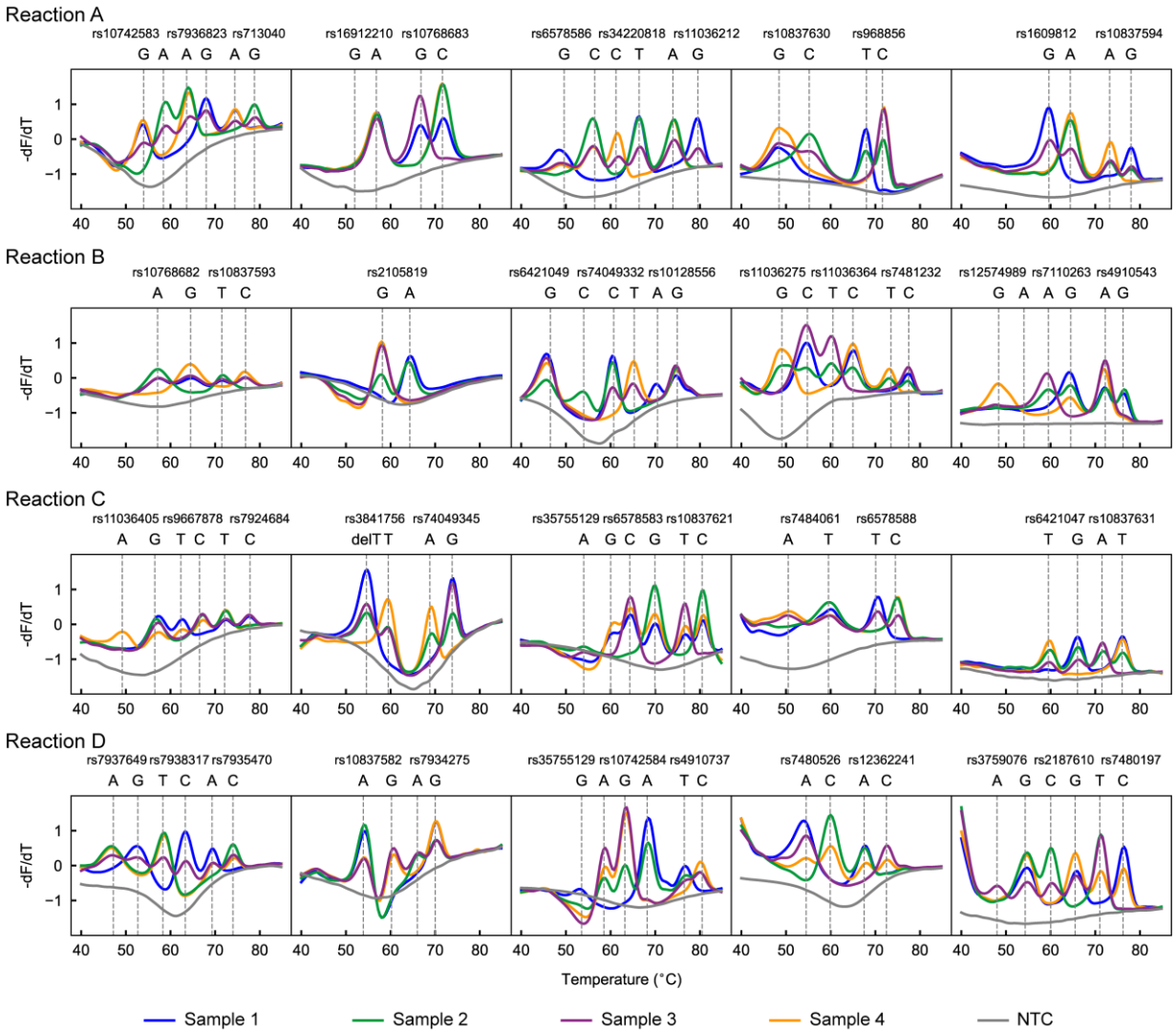


Figure S2 Representative multicolor melting curve analysis profiles for the 48 *HBB*-flanking SNPs.

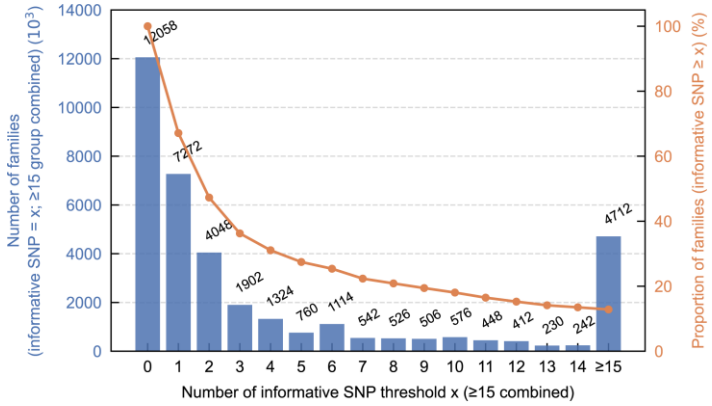


Figure S3 Distribution of informative SNP numbers in simulated families based on 36,672 ordered parental pairings generated from 192 unrelated individuals, based on the 48 SNPs flanking *HBB*.

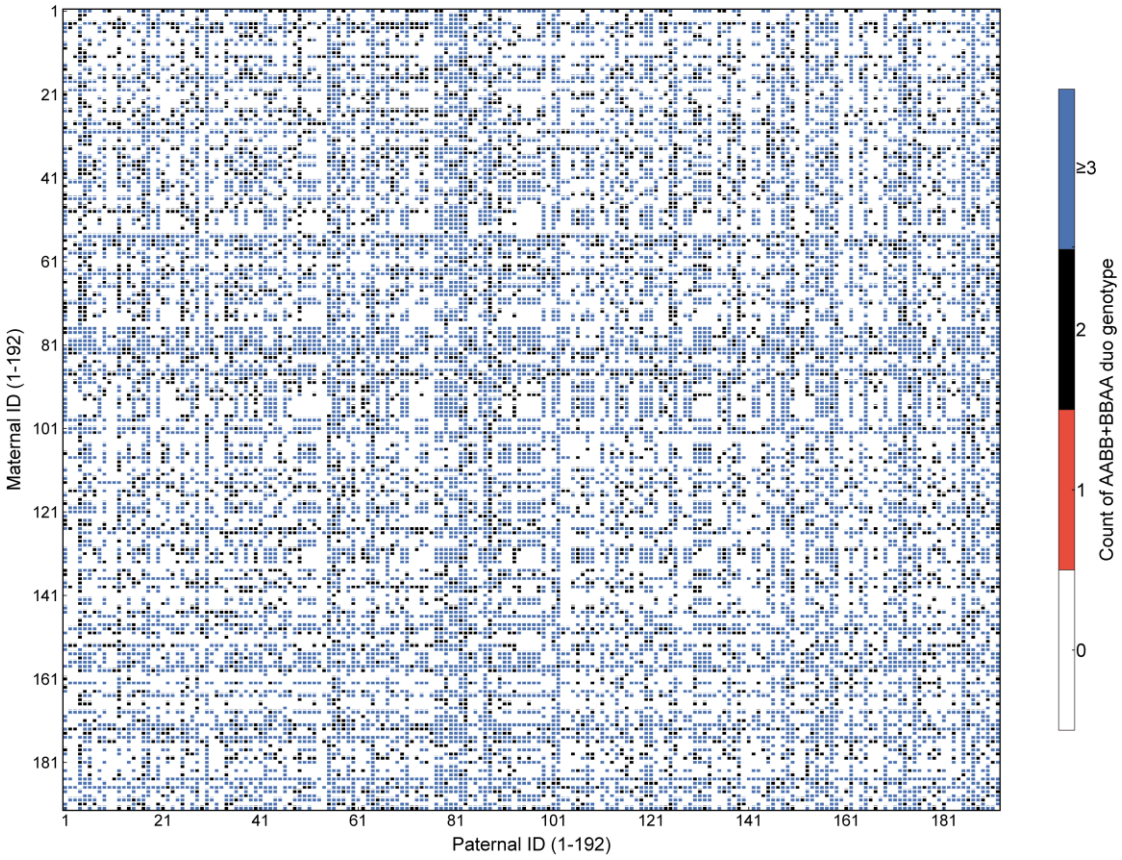


Figure S4 Heatmap of informative SNP numbers for AABB and BBAA genotype configurations in simulated 36,672 parental duo families generated by pairing 192 paternal and 192 maternal samples, based on the 48 SNPs flanking *HBB*.

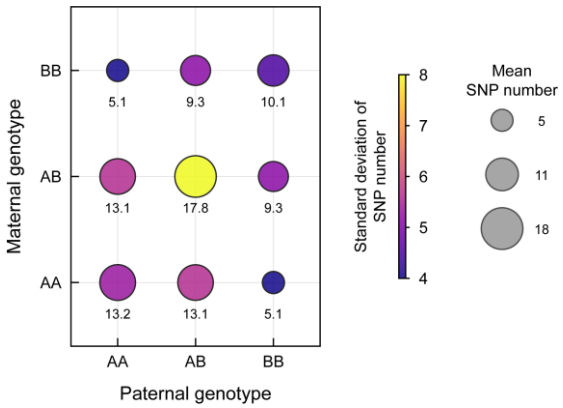


Figure S5 Bubble plot of informative SNP numbers across nine parental genotype combinations in simulated duo families. The plot was generated from two SNP panels: 48 SNPs flanking *HBB* and 48 genome-wide autosomal SNPs. Informative-SNP numbers across nine parental genotype combinations were analyzed in simulated parental duo families generated from 192 paternal and 192 maternal samples.



Figure S6 Representative singleplex Drop-Phase assay results for the 48 *HBB*-flanking SNPs. Each SNP-specific probe carries a single fluorophore (FAM or HEX), whereas mutation-specific probes are available with both fluorophores. For a duplex dPCR

phasing assay, the SNP probe is paired with the mutation probe bearing the opposite fluorophore, allowing flexible determination of linkage between the SNP and the mutation.

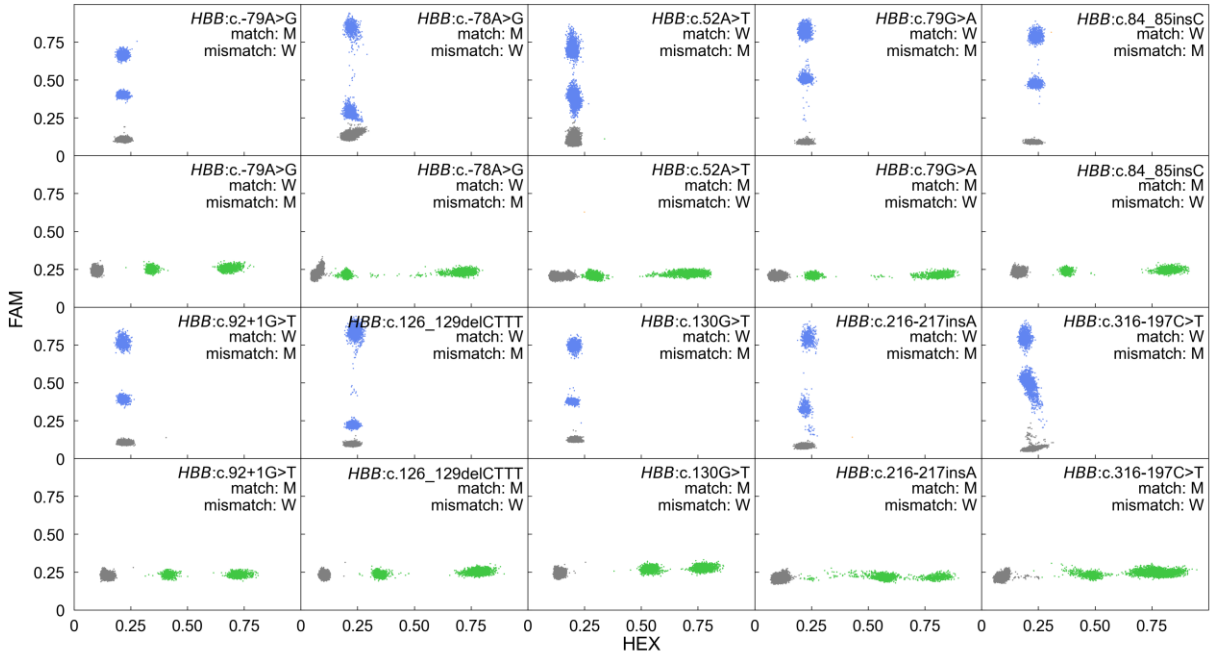


Figure S7 Representative singleplex Drop-Phase assay results for β-thalassemia mutations. Each mutation was detected with both FAM- and HEX-labeled probes. In a duplex dPCR phasing assay, the mutation probe carrying the fluorophore opposite to that of the SNP probe is selected, allowing the mutation to be paired with any SNP regardless of the SNP probe fluorescence channel.

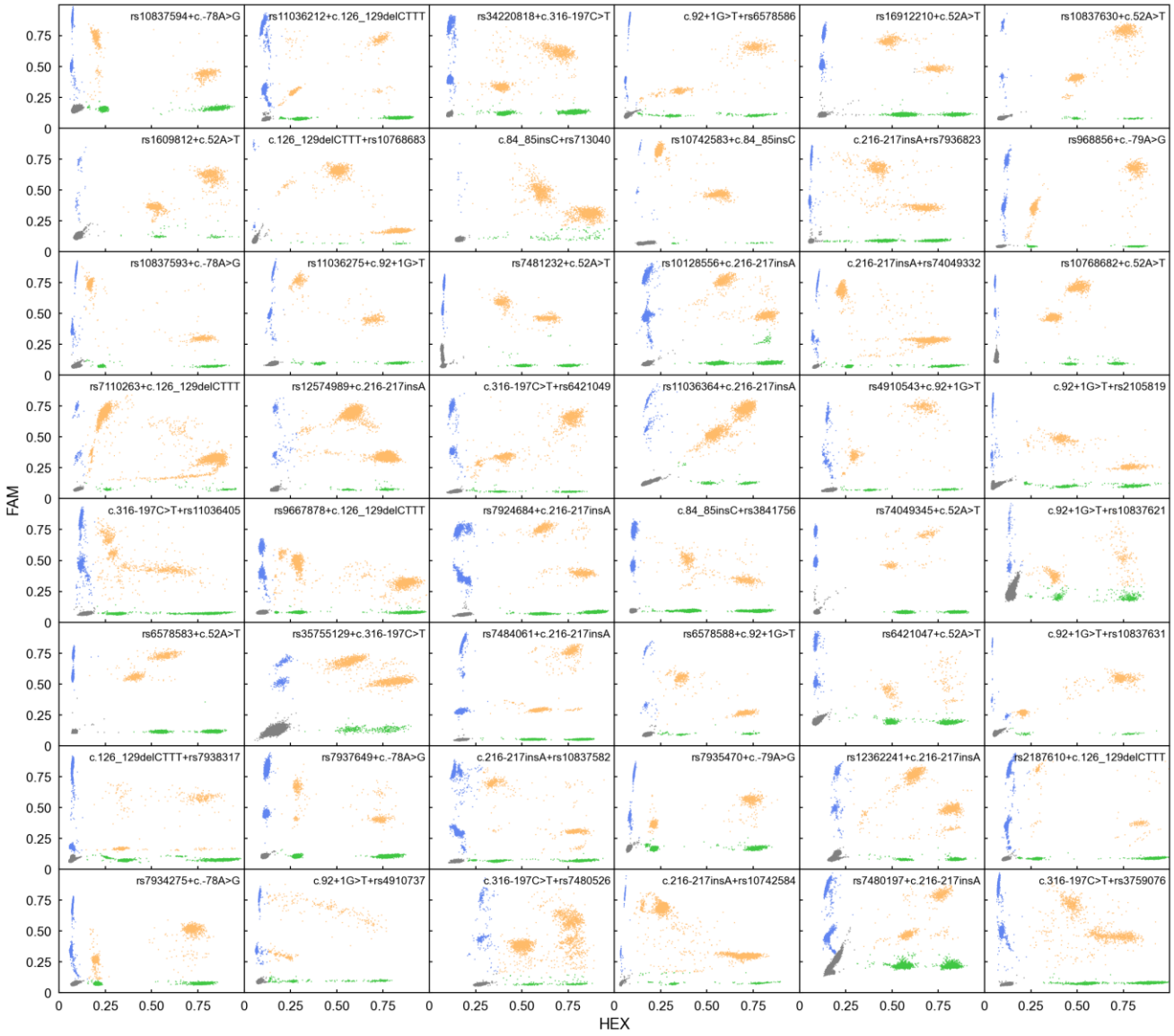


Figure S8 Representative Drop-Phase assay results for 48 SNPs paired with a β-thalassemia mutation. In each duplex assay, the two loci are named sequentially: the first locus is detected in the FAM channel and the second locus in the HEX channel. This naming convention applies to all SNP–mutation combinations.

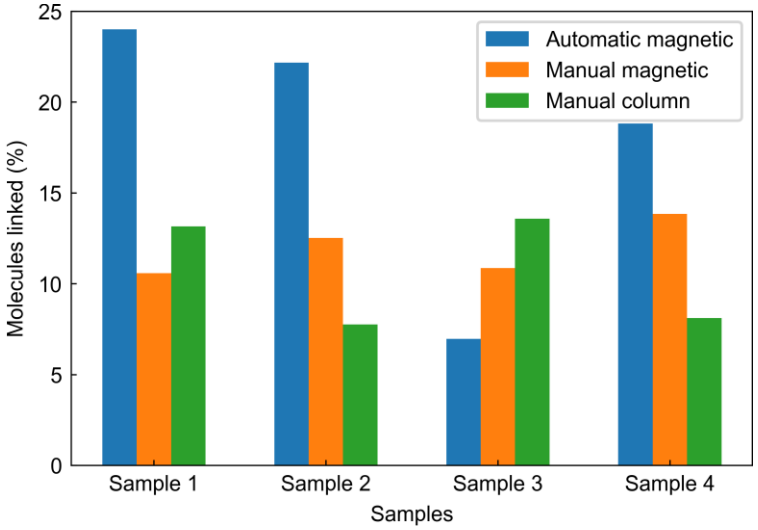


Figure S9 Effect of gDNA extraction workflow on the proportion of linked molecules. Three extraction strategies were assessed: automated magnetic bead-based extraction using the Lab-Aid 824 system (Zeesan Biotech, Xiamen, China), manual magnetic bead extraction (Zeesan Biotech) and column-based extraction (CWBIO, Jiangsu, China). In four independent individuals, linkage between two chromosome 11 SNPs, rs968856 and rs6421049, separated by approximately 26.5 kb, was quantified to estimate the proportion of DNA fragments long enough to support physical linkage analysis.

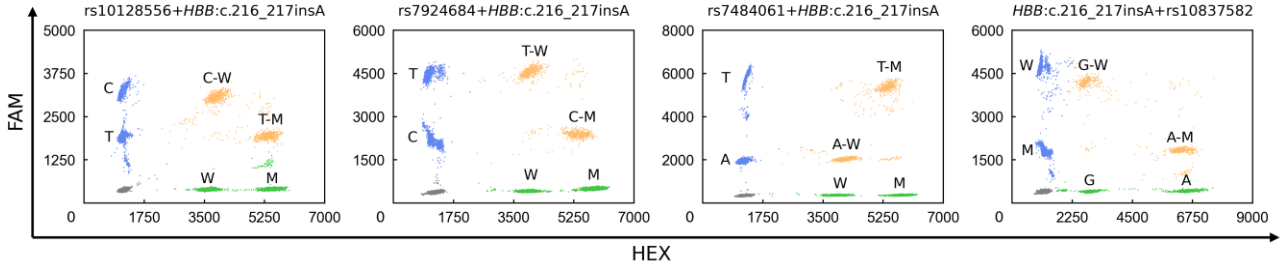


Figure S10 Drop-phase analysis of linkage between β-thalassemia mutation and *HBB*-flanking SNPs in a validation family.

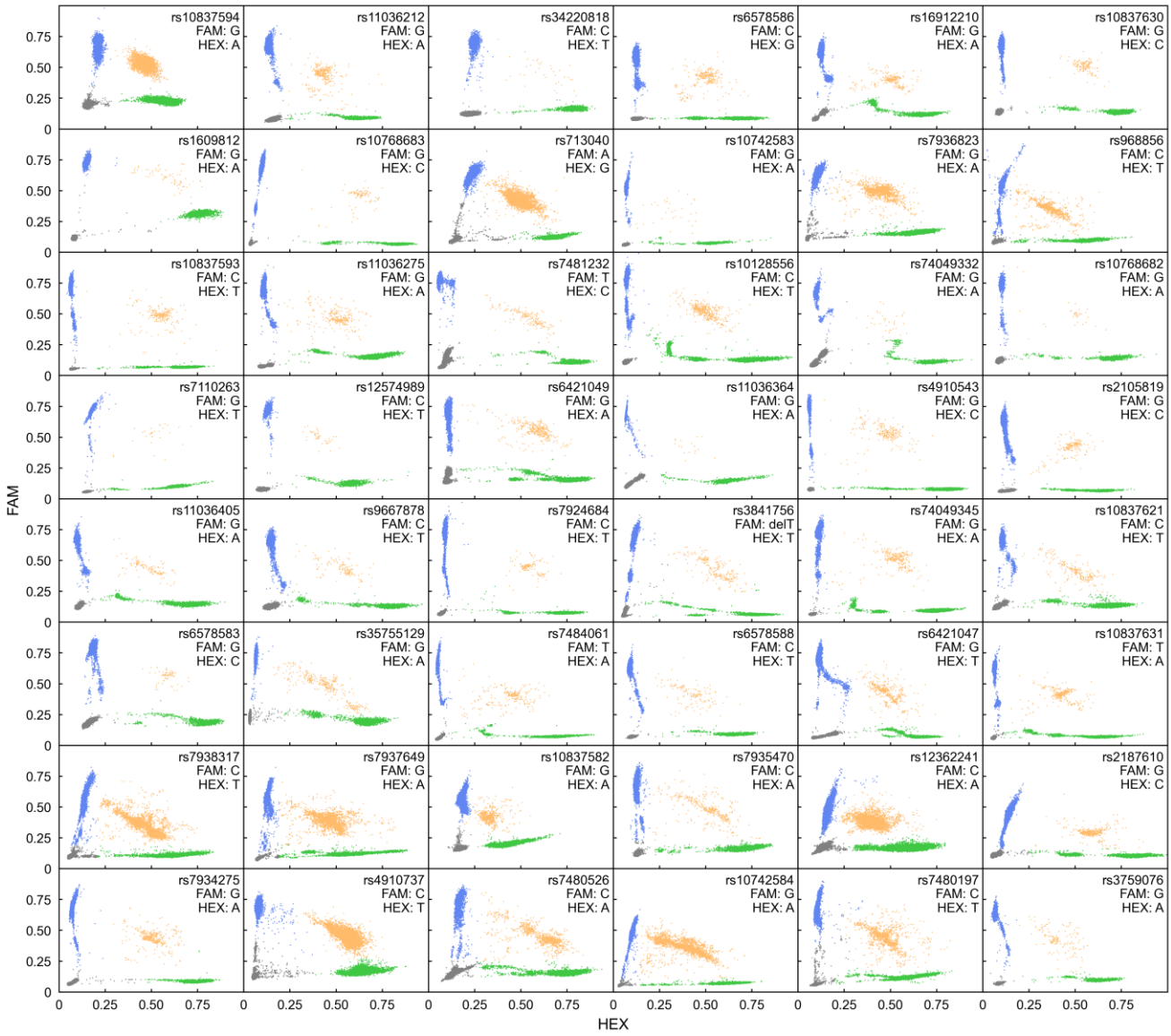


Figure S11 Representative allele quantification results for the 48 *HBB*-flanking SNPs.

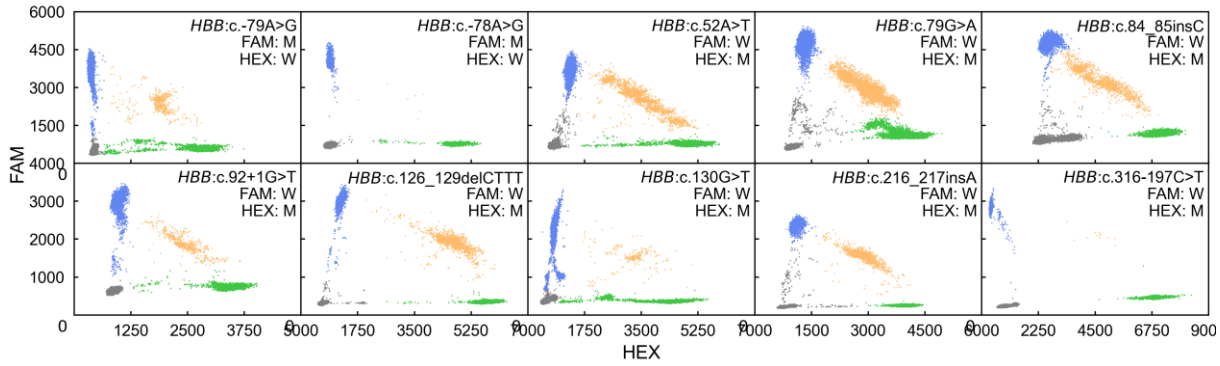


Figure S12 Representative allele quantification results for 10 β-thalassemia mutations.

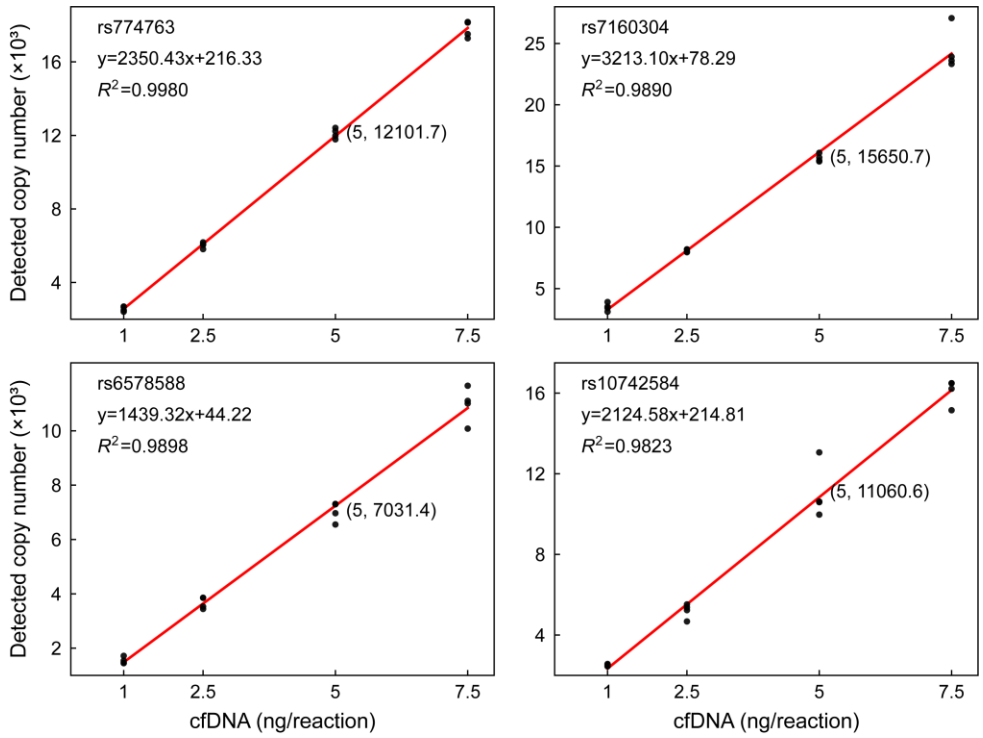


Figure S13 Correlation between detected copy number and input DNA amount.

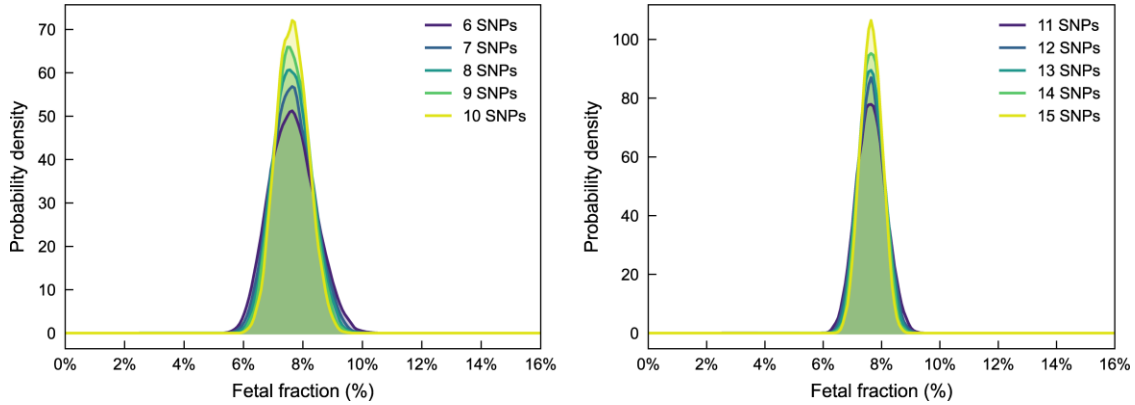


Figure S14 Density distributions of fetal fraction estimates using 6–15 informative SNPs. Kernel density curves of mean fetal fraction were obtained from 10,000 random subsamples without replacement from the original 29 SNPs for each SNP number (n = 6–15).

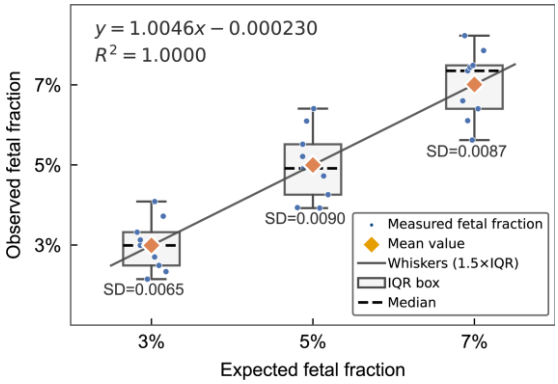


Figure S15 Linear regression analysis of fetal fraction measurement. Fetal fraction was calculated from nine qualified fetal fraction informative SNPs (FF-iSNPs). Box plots show the distribution of measured fetal fractions (n = 9 per group), with the horizontal black line indicating the median, boxes spanning the interquartile range (IQR) and whiskers extending to 1.5× IQR. Orange diamonds represent the grand mean of all combinations and were used for linear regression fitting (solid grey line). The regression equation and coefficient of determination (R^2) are shown in the upper left corner. Standard deviation (SD) values are annotated next to the corresponding mean values.

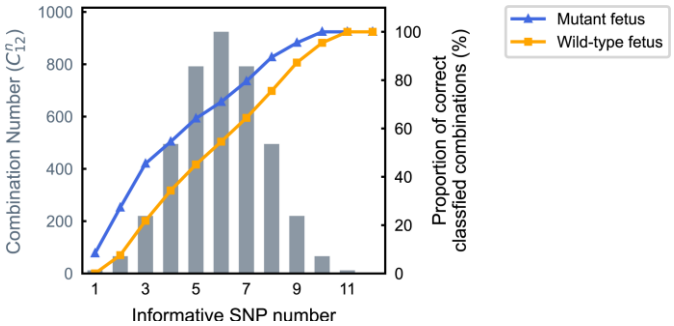


Figure S16 Locus-combination (robustness) analysis of the relationship between informative SNP number and maternal mutation classification under 5 ng cfDNA input, at 3% fetal fraction. Grey bars show the number of possible combinations as a function of informative SNP number (n), with the maximum number of combinations occurring at n = 6. Overlaid lines show the proportion of combinations classified correctly, defined as combinations reaching the decision boundary that corresponds to the reference fetal genotype (below −4.595 for wild-type fetal standards and above 4.595 for mutant fetal standards); combinations reaching the opposite boundary were scored as misclassifications and those reaching neither boundary as inconclusive. These combinations are resampled from the same loci and therefore do not represent independent samples.

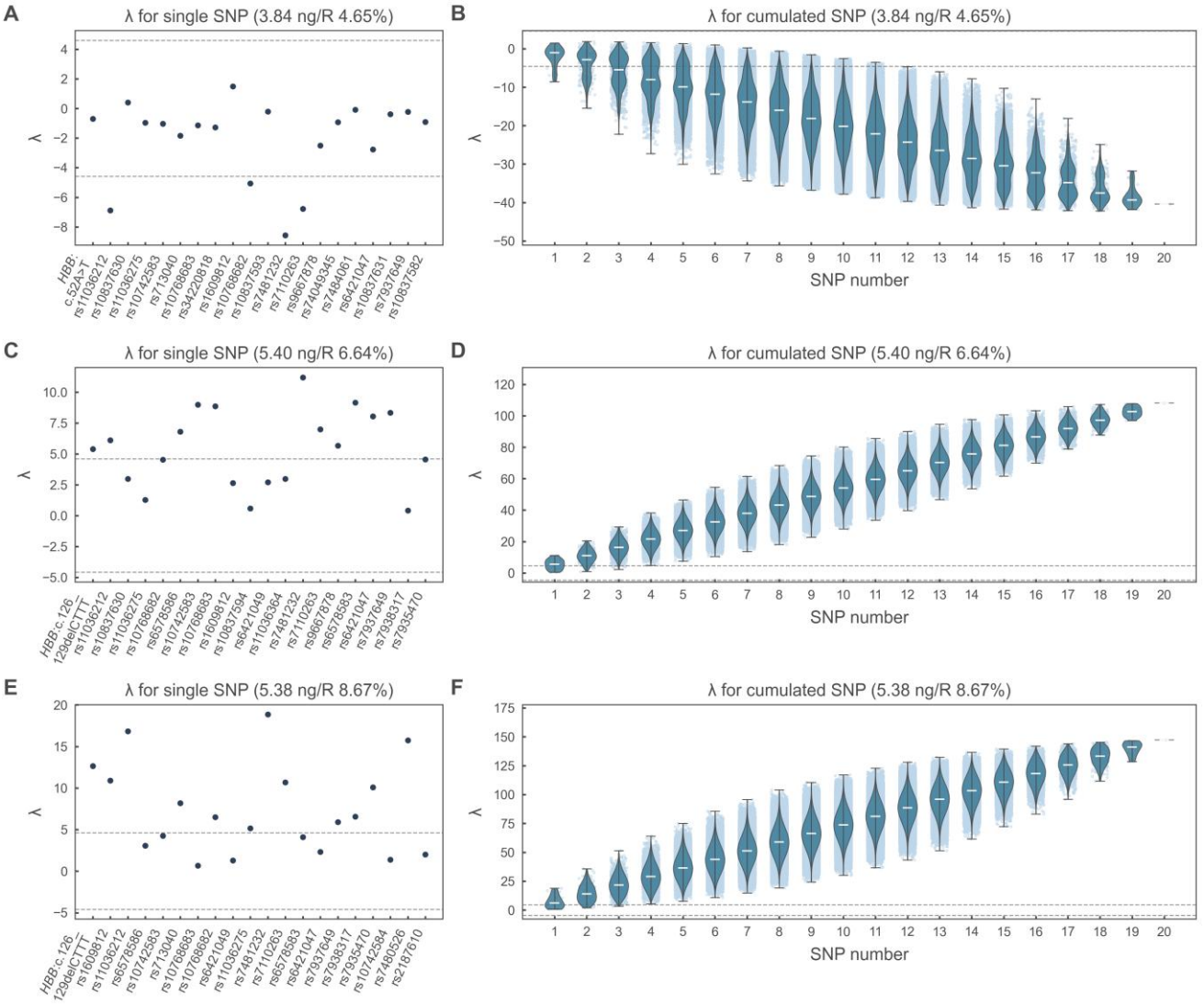


Figure S17 Sequential probability ratio test (SPRT)-based maternal mutation classification in three clinical samples. Single-locus (A, C, E) and cumulative multi-locus SPRT analyses (B, D, F) are shown for samples with 4.65% fetal fraction and 3.84 ng cfDNA input, 6.64% fetal fraction and 5.40 ng cfDNA input, and 8.67% fetal fraction and 5.38 ng cfDNA input, respectively.

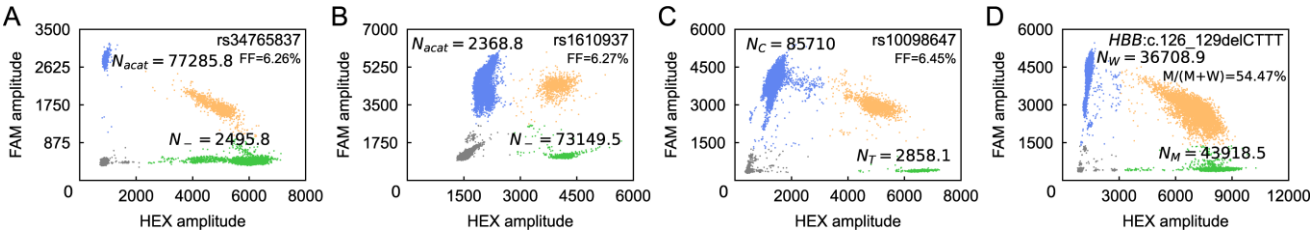


Figure S18 dPCR-based allele quantification of fetal fraction–informative loci and *HBB*:c.126_129delCTTT in family Sample-59. FF, fetal fraction; N, detected copy number of each allele.

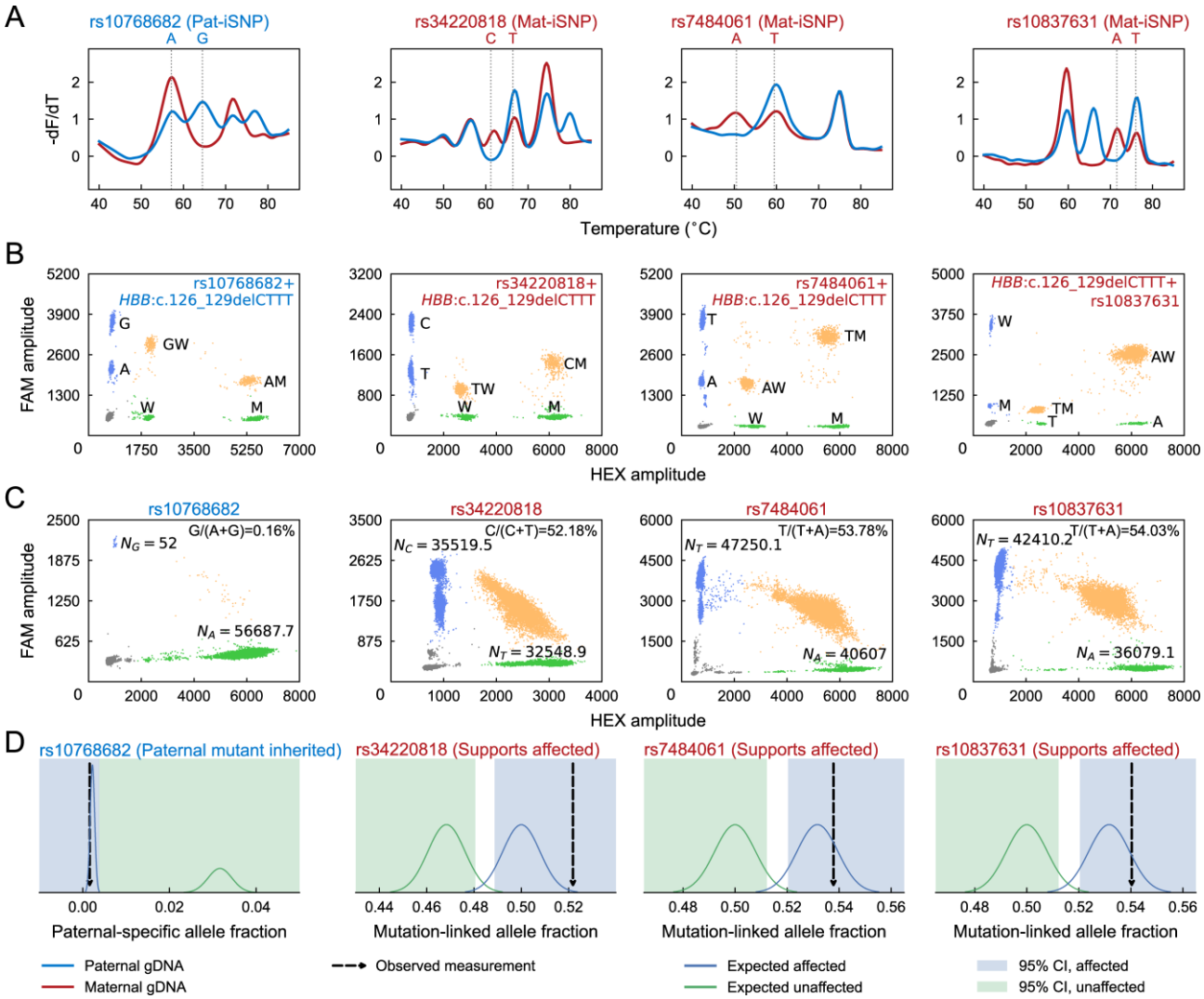


Figure S19 Integration of MMCA, Drop-Phase, and allele quantification assay for clinical inference in a representative family (Sample-59). (A) MMCA-based genotyping of one paternally informative SNP (Pat-iSNP) and three maternally informative SNPs (Mat-iSNPs). Genotypes are annotated above corresponding melting peaks. (B) Drop-Phase linkage analysis across SNP loci and *HBB* mutations, distinguishing maternal (M) and wild-type (W) haplotypes. In each duplex assay, the two loci indicated on the upper right corner are designated in order: the first is detected in the FAM channel, and the second in the HEX channel. (C) dPCR-based allele quantification of SNP loci, showing absolute copy numbers (N) for each allele. (D) Statistical classification of fetal inheritance using log-likelihood ratio frameworks. Dotted arrows indicate allele fractions used for inference. Blue and green shaded regions represent classification boundaries for paternal and maternal inheritance.

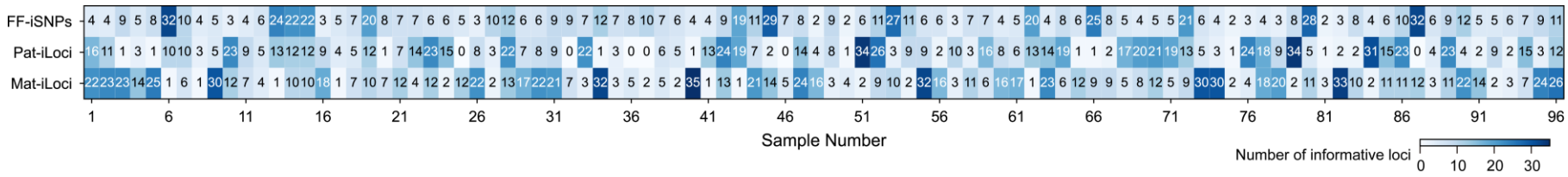

FF-iSNPs
Pat-iLoci
Mat-iLoci
1
6
11
16
21
26
31
36
41
46
51
56
61
66
71
76
81
86
91
96
Sample Number
Number of informative loci
0
10
20
30

Figure S20 Distribution of informative loci across 96 clinical samples. FF-iSNPs, fetal fraction informative SNPs; Pat-iLoci, paternally informative loci; Mat-iLoci, maternally informative loci.

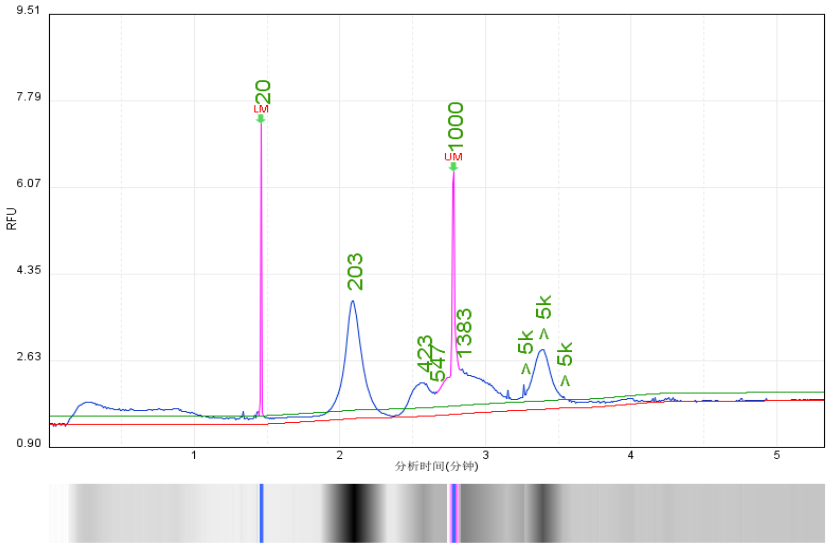


Figure S21 The capillary electrophoresis result of Sample-56 cfDNA (FF=2.31%).